Enhancing Oil Recovery in Vertical Heterogeneous Sandstone Reservoirs Using Low-Frequency Pulsating Water Injection

Osmund Edward Mwangupili * and Chunsheng Pu

Posted Date: 11 December 2024

doi: 10.20944/preprints202412.0942.v1

Keywords: low-frequency; oil recovery; vertical heterogeneity; oil mobility; water channelling

 doi:10.20944/preprints202412.0942.v1

Article

Enhancing Oil Recovery in Vertical Heterogeneous Sandstone Reservoirs Using Low-Frequency Pulsating Water Injection

Osmund Mwangupili * and Pu Chunsheng

China University of Petroleum-East China, Qingdao, 266580, China
* Correspondence: osmund94@gmail.com

Abstract: Enhanced oil recovery (EOR) techniques, such as water flooding, often face significant challenges in heterogeneous reservoirs, mainly due to permeability variations that hinder effective oil displacement. This study investigated the impact of pulsating water flooding on oil recovery in reservoirs with vertical heterogeneity, focusing on interlayer and inlayer permeability variations. Laboratory experiments were conducted using cylindrical sand pack models with varying permeability to compare steady-state and pulsating water injection methods. The results demonstrated that pulsating water flooding significantly improved vertical sweep efficiency (VSE) and overall oil recovery, particularly in low-permeability zones. Pulsations helped mobilize trapped oil and redistributed injected water more evenly, mitigating the adverse effects of early water breakthrough and enhancing sweep efficiency. For interlayer heterogeneity, pulsating water injection increased total recovery by 23.2%, 8.9%, and 6.6% for core groups with permeability ranges of 307.9 × 10^{-3} μm², 193.9 × 10^{-3} μm², and 73.25 × 10^{-3} μm², respectively. For inlayer heterogeneity, recovery factors improved by 13.9%, 10.6%, and 3.1%, respectively. Core groups with higher permeability ranges (i.e., larger differences between high and low permeability) experienced lower recovery under steady-state conditions; while pulsating injection mitigated these effects, resulting in higher recovery in more heterogeneous reservoirs than steady-state flooding. These findings suggest that pulsating water flooding is an effective and cost-efficient technique for enhancing oil recovery in heterogeneous reservoirs. It improves short-term and long-term recovery by increasing displacement efficiency, particularly in low-permeability regions, and effectively mitigates the challenges of permeability variations. As such, pulsating water flooding offers a significant improvement over steady-state flooding, providing valuable insights for EOR practices in complex reservoirs.

Keywords: low-frequency; oil recovery; vertical heterogeneity; oil mobility; water channelling

1. Introduction

Global energy demand is rising due to industrial growth and technological reliance, making enhanced oil recovery (EOR) technology essential for efficient oil extraction. EOR plays a crucial role in addressing energy shortages and ensuring a sustainable supply of crude oil and natural gas, supporting long-term energy security [1–5].

While renewable energy expands, oil remains crucial for developing regions and energy-intensive industries. As new reserves become more challenging, maximizing recovery from existing reservoirs is essential. Due to geological limitations, conventional methods often leave significant oil trapped [5]. The permeability of common geologic media varies significantly, spanning approximately 16 orders of magnitude. This variation ranges from extremely low permeability values, as low as 10^{-23} m² in intact crystalline rocks, shales, and fault cores, to much higher values of 10^{-7} m² in well-sorted gravels. This broad range highlights the **heterogeneity** of subsurface

 doi:10.20944/preprints202412.0942.v1

environments and underscores the importance of understanding permeability when analyzing fluid flow and recovery processes in different geological formations.

Sandstone reservoirs are a significant type of reservoir characterized by their extensive distribution and abundant reserves. Geological processes such as sedimentation, diagenesis, and tectonic activity play a crucial role in their development, resulting in spatial variability and non-uniform reservoir characteristics [6,7]. A notable feature of sandstone reservoirs is the presence of multiple oil-bearing layers formed during deposition. Variations in depositional environments cause differences in key parameters such as thickness, porosity, and permeability among these layers, contributing to the reservoir's vertical heterogeneity. This vertical variability significantly influences fluid distribution and movement within the reservoir, posing challenges for enhanced oil recovery (EOR) techniques like water flooding.

Reservoir heterogeneity, a significant challenge in oil-bearing formations, impacts the effectiveness of water flooding, which is commonly used to enhance oil recovery [8]. This heterogeneity arises from sedimentation, lithification, and structural processes, leading to spatial differences in rock types, fluid properties, and physical characteristics that influence fluid flow. Researchers classify heterogeneity by factors such as scale, depositional characteristics, and its impact on fluid behaviour, helping to quantify and manage its effects on fluid flow in the reservoir [9]. Vertical sweep efficiency, a key measure of waterflooding success, refers to the proportion of the reservoir's vertical cross-sectional area between injection and production wells effectively reached by injected water at a given time [8].

Vertical heterogeneity in sandstone reservoirs can be further categorized into two main types: interlayer and in-layer heterogeneity. Interlayer heterogeneity refers to differences between distinct layers, often caused by large-scale changes in the depositional environment, such as a shift from coarse-grained sandstone to fine-grained shale. These differences result in varying permeability, porosity, and fluid saturation levels across layers. In contrast, in-layer heterogeneity refers to variations within a single layer arising from factors like changes in grain size, local sedimentary conditions, fractures, or other features that affect fluid flow. Interlayer heterogeneity is a widespread characteristic of multi-layer sandstone reservoirs commonly observed in oilfields [10]. Both types of heterogeneity influence fluid flow and recovery efficiency, making it crucial to understand and manage these variations to optimize water flooding and enhance oil recovery.

In China, where most oilfields have entered mid-to-late development stages, characterized by production decline and reduced recovery efficiency, heterogeneity challenges have intensified [9]. Variations in matrix permeability, both horizontally and vertically, significantly affect water flooding performance, leading to issues such as water channeling through oil zones, which causes certain areas to be bypassed (areal sweep problem), and early water breakthrough in high-permeability zones, which leaves oil trapped in low-permeability areas (vertical sweep problem) [11,12]. Water channeling, in particular, remains a significant issue due to strong vertical heterogeneities in continental clastic rocks, which account for 92% of the total reservoir rocks in China. This issue is compounded in fields with water cuts frequently exceeding 90%, with some mature fields reaching up to 98%, indicating that traditional water flooding methods are no longer sufficient to meet EOR demands [9,13].

The adverse effects of heterogeneity are worsened when the displacing fluid (water) has higher mobility than the displaced fluid (oil), leading to a preferential flow path and reduced displacement efficiency [14]. Factors such as the mobility ratio, injection rate, reservoir heterogeneity, rock permeability, and capillary and gravitational forces all influence oil displacement efficiency [15–17]. Medium-permeability sandstone reservoirs, characterized by varied pore structures and fluid flow dynamics, present unique challenges for EOR and demand strategies that address these heterogeneities to optimize recovery [18].

To address these challenges, advanced EOR methods that account for reservoir heterogeneity have been explored, including polymer flooding, chemical flooding, gas injection, and thermal recovery. Each of these methods, however, has limitations when applied to reservoirs with significant

 doi:10.20944/preprints202412.0942.v1

heterogeneity. In contrast, pulsating water injection offers a unique solution by utilizing pressure fluctuations to improve oil recovery.

This technique introduces low-frequency hydraulic pulses to improve oil mobilization and sweep efficiency in heterogeneous reservoirs. Inspired by observations of increased oil recovery following seismic activity, the approach applies energy to induce reservoir vibrations that modify the porous media and improve the seepage capacity of reservoir rocks [19–25]. One of the advantages of pulsating water injection is its ability to enhance existing infrastructure with minimal additional components, making it a cost-effective solution [26–31].

By introducing pressure fluctuations, pulsating waterflooding enhances oil recovery by dislodging and coalescing oil droplets in pore throats, which enables faster fluid flow, reduces displacement time, and addresses heterogeneity challenges within the reservoir [32–36]. Pulsating waterflooding improves sweep efficiency by creating abrupt, oscillating forces at the pore level, which can bypass preferential flow paths, especially in high-permeability zones, and improve fluid distribution across the reservoir. Pressure pulsing can mobilize trapped oil droplets by overcoming capillary blockages and combining them into larger, more mobile droplets, further enhancing recovery efficiency [19].

In this study, we investigated the use of low-frequency pressure fluctuations to enhance vertical displacement efficiency in reservoirs with interlayer and inlayer permeability heterogeneity. Double cylindrical sand pack models were used to simulate reservoirs with varying permeability ratios, mimicking real-world conditions. By applying low-frequency fluid pulsing in saturated media, these fluctuations enhanced flow instabilities, which helped bypass preferential flow paths in high-permeability zones, a common issue in conventional water flooding. Pulsating water injection redistributed flow more evenly, improving fluid mobility in low-permeability zones that are difficult to reach with conventional flooding. This dynamic flow environment, driven by oscillating forces, increased the flow rate and allowed the injected water to reach previously bypassed areas in both high and low-permeability regions, thereby enhancing oil recovery.

The relationship between permeability range, oil recovery, and water injection flow behaviour in high- and low-permeability layers was carefully examined. The results highlighted that the effectiveness of pulsating injection depended on the permeability characteristics of each layer, with high-permeability zones showing reduced water breakthrough and low-permeability zones revealing improved oil displacement. The study demonstrated that low-frequency pulsating water injection effectively improves oil recovery in heterogeneous reservoirs. The results provided valuable insights into how pressure pulsing enhances recovery by addressing the challenges posed by complex permeability variations, thus advancing enhanced oil recovery (EOR) strategies.

2. Materials and Methods

2.1. Materials

2.1.1. Experimental Core

All cores were manufactured in cylindrical sand packs with φ 2.5 cm and 40 cm length, with the calculated volume of a single pack being 196.35 mL. Quartz sands with mesh numbers (40, 60, and 80) were prepared in a 1:1:1 volume ratio. The cells were packed with sand and subjected to 1 MPa axial stress. The experimental cores were explicitly designed to match the properties of the BZX oilfield, with an average porosity of 26.7% and an average permeability of 320.7×10^{-3} μm². According to the porosity distribution of the BZX Oilfield, the porosity ranges from 1.3% to 33.9%, and the permeability ranges from 10.1×10^{-3} to 1040.9×10^{-3} μm².

To produce artificial cores with varying permeability, cylinders with a φ 2.4 cm and varying lengths were used in conjunction with an artificial core production device made by Jiangsu Hongbo Machinery Manufacturing Co., Ltd. The artificial cores were formed by repeatedly inserting the smaller diameter cylinders into the sand pack and compacting the sand until the core was fully formed. Figure 1a,b show artificial core devices (sand packs) and core-making devices. A total of 24

 doi:10.20944/preprints202412.0942.v1

artificial cores were created in six groups, with both high and low-permeability cores in each group to ensure consistency.

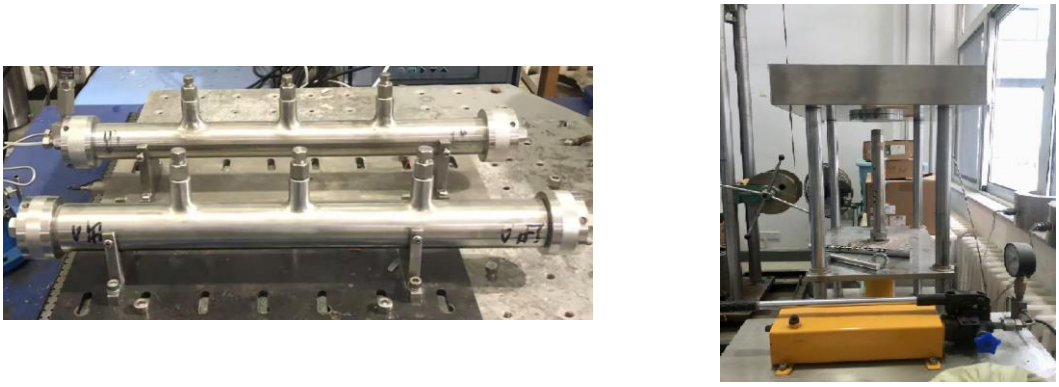

(**a**) (**b**)

Figure 1. Experimental core manufacturing equipment (a) Sand pack models (b) Core making device.

2.1.2. Fluid System

The fluids used in this study included de-ionized water, simulated water, and simulated oil, with viscosities measured using a standard viscometer, as shown in Figure 2a. The simulated water was prepared by mixing deionized water with 3% KCl and stirring it using a cantilever-type electric stirrer, operating at speeds ranging from 50 to 3000 rpm, provided by Lichen Technology Co., Ltd., as shown in Figure 2b. This process resulted in a viscosity of 1.28 mPa.s at 25 °C. In the study area, the average viscosity of crude oil was 24.76 mPa.s at 50 °C. To create the simulated oil, 150 mL of high-viscosity crude oil (5000 mPa.s) was mixed with 90 mL of kerosene (1.78 mPa.s), resulting in a viscosity of 24 mPa.s at 25 °C and 0.1 MPa.

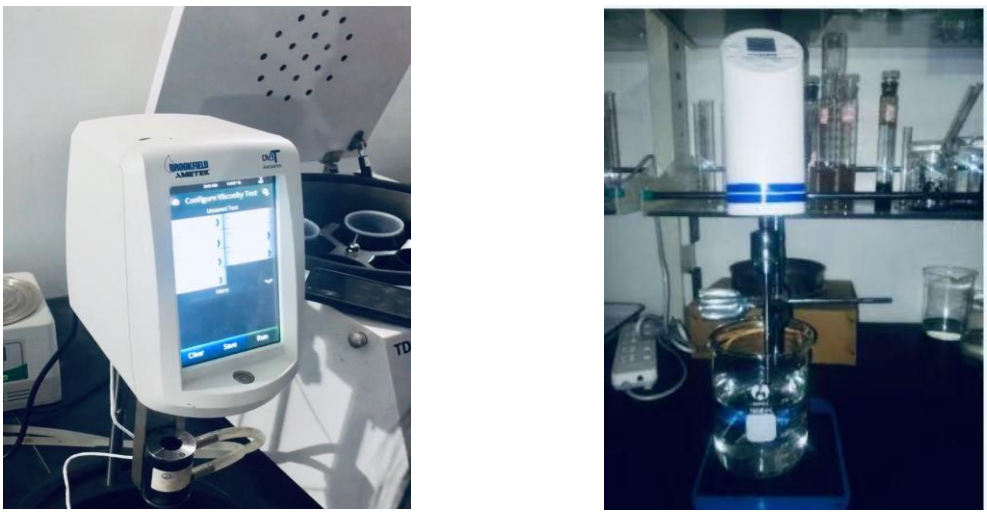

(**a**) (**b**)

Figure 2. Experimental devices (a) Standard viscometer (b) Cantilever-type electric stirrer.

2.1.3. Injection System

The flow of fluids through the sand pack models was controlled by the AB pump, with a flow rate of 1 mL/min. The 1 mL/min flow rate was chosen to simulate the typical seepage velocity observed in reservoir conditions. This rate was calculated using Darcy's law, considering factors such as the permeability, porosity, pressure difference, and cross-sectional area of the sand pack models, which were designed to replicate the characteristics of reservoir rocks. The calculated flow rate was

 doi:10.20944/preprints202412.0942.v1

0.97 mL/min, and a target flow rate of 1 mL/min was chosen to ensure consistency and minimize experimental errors.

To maintain a constant mass flow rate, we employed several strategies. First, the AB pump was precisely calibrated and continuously monitored to ensure it maintained a stable flow rate. A commercial data acquisition system was used to record flow and pressure data from pressure transducers, with real-time monitoring provided by the Easy Sense® 2100 software. The pressure measurements were taken using Trafag NAT 8252 transducers, allowing for close control over system pressure and flow behaviour.

For pulsating water injection, pressure pulses were generated using a solenoid valve (NASS 0545 00.1-00 BV 5802 model) with a digital timer relay box. The fluids were injected via high-pressure stainless-steel transfer cylinders to minimize flow fluctuations rather than directly through the pump. This setup ensured that pressure and flow rate were precisely controlled while protecting the pump from potential damage or clogging due to pressure spikes or particulate matter in the fluids.

By utilizing a combination of precise flow control, regular monitoring, and careful calibration, we maintained a consistent mass flow rate throughout the experiment, ensuring reliable and repeatable results while minimizing experimental error.

2.1.4. Experimental Uncertainty

The uncertainty in the experimental measurements was estimated to be ±5% based on repeated trials. The error variation was primarily due to minor inconsistencies in sand packing and fluid injection rates.

2.2. Methodology

This research studied two types of reservoir vertical heterogeneity: interlayer and inlayer heterogeneities. To address the challenges associated with these forms of reservoir heterogeneity, the study investigated the application of low-frequency pulsating water injection in medium-permeability sandstone reservoirs. Parallel sand pack models, composed of high- and low-permeability sand packs (φ 2.5 cm × 40 cm), were utilized to simulate reservoir heterogeneity.

To simulate interlayer heterogeneity, the inlets of low and high-permeability sand packs were arranged in parallel. On the other hand, inlayer heterogeneity was simulated by combining the outlets along the length of low and high-permeability sand packs.

Figures 3 and 4 show the schematic diagrams of the experimental setups used in this research. All experiments were conducted at a controlled temperature of 25 °C (77 °F) and under atmospheric pressure of 0.1 MPa to ensure consistency and reproducibility. The experimental workflow involved the following steps:

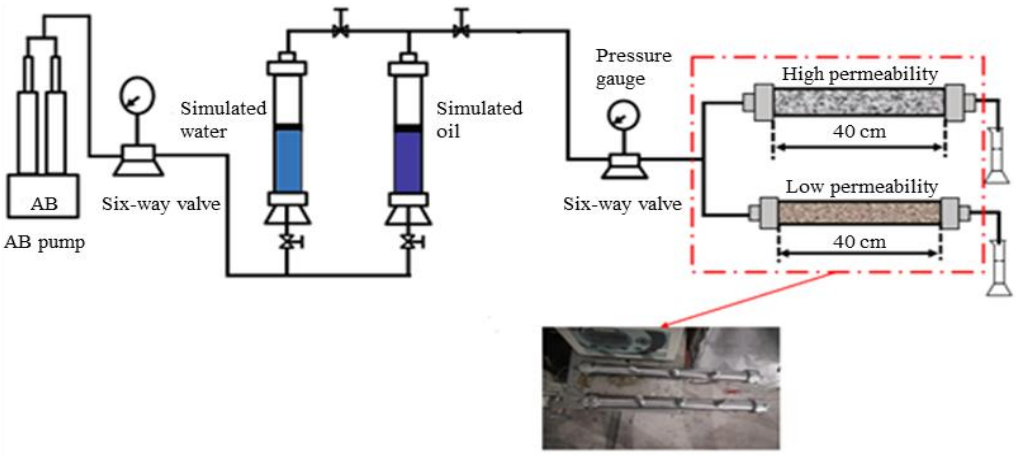

Figure 3. The schematic diagram of vertical interlayer heterogeneity water flooding simulation.

 doi:10.20944/preprints202412.0942.v1

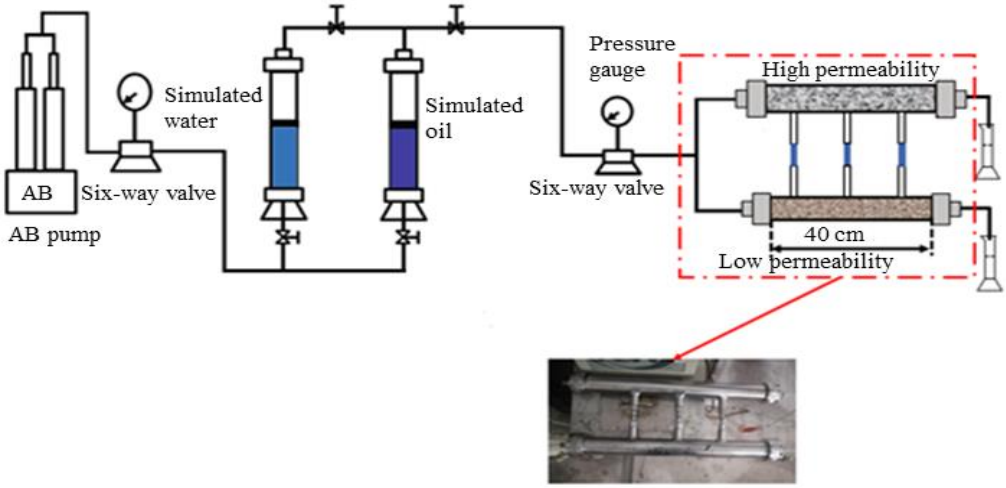

Figure 4. The schematic diagram of vertical inlayer heterogeneity water flooding simulation.

The experiments involved three main phases: core saturation with simulated water to establish connate water saturation, initial oil saturation, and water flooding. De-ionized water, simulated water, and simulated oil were separately placed into transfer cylinders. The dry weight of each core was measured before connecting it to displacement equipment. The core was then saturated with simulated formation water injected at a 1 ml/min flow rate for 8 hours to mimic seepage flow conditions.

After the core was saturated with simulated water, its wet weight was recorded, from which the pore volume and porosity were calculated. The permeability of each sand pack was then determined using Darcy's law based on the flow data obtained during the experiment.

Simulated oil was injected into each core until irreducible water saturation was reached, with more than 10 pore volumes (PV) of oil injected into each model. Afterwards, the models were left idle for 8 hours to stabilize pressure. Following this, steady-state and pulsating water flooding experiments were conducted. For steady-state water flooding, a solenoid valve was opened, while for pulsating water injection, the solenoid valve's switching time was adjusted (frequency of 1 Hz, amplitude of 1 MPa) [30]. Over 20 PV of simulated water was injected into each model, and the liquid output was recorded every 2 minutes for the first 20 minutes. The experiments were terminated when the water cut reached 98%. Injected and produced oil volumes were measured during both water flooding stages to calculate the final oil displacement efficiency.

3. Experimental Results and Discussions

We present the results of waterflooding experiments conducted in two vertical heterogeneity environments: interlayer and inlayer heterogeneities. The experiments demonstrated that pulsating waterflooding enhances fluid flow and oil recovery in vertical heterogeneity environments. Conventional waterflooding was performed to set the baseline for comparison with pulsating injection [37].

In these experiments, the goal was to assess the impact of hydraulic pulsations on fluid flow through these heterogeneous layers. The dual sand pack models provided valuable insights, highlighting that pulsating water injection has the potential to mobilize trapped oil in lower permeability zones more effectively than the steady-state injection, suggesting an advantage of pulsation in improving sweep efficiency within heterogeneous formations [18].

In vertically heterogeneous reservoirs, geological variations between layers or sand bodies, often shaped by the sedimentary environment, significantly impact fluid storage and flow dynamics. Such variations, particularly in permeability, influence waterflooding performance, leading to common challenges like monolayer breakthrough, interlayer interference, and imbalanced injection and production rates [38].

 doi:10.20944/preprints202412.0942.v1

Research in multilayer reservoirs has demonstrated that fluid production can vary considerably across layers due to vertical heterogeneity, with single-core and combined-core models revealing how these variations affect water distribution and sweep efficiency during waterflooding [39–42]. Table 1 shows the physical properties of the experimental cores used in this research.

Table 1. Physical Properties of Experimental Cores.

Core	Diameter cm	Length cm	Relative Permeability	Dry weight g	Porosity %	Permeability x10^{-3} μm^2
2-1	2.5	40	Low	398.8	26.0	35.7
	2.5	40	High	398	31.9	348.5
	2.5	40	Low	398.7	25.8	34.8
	2.5	40	High	398.1	31.5	337.8
2-2	2.5	40	Low	398.4	30.3	127.4
	2.5	40	High	397.9	31.3	318.9
	2.5	40	Low	398.5	29.5	125.4
	2.5	40	High	398.3	31.0	321.7
2-3	2.5	40	Low	398.9	29.4	251.8
	2.5	40	High	398.4	31.7	327.3
	2.5	40	Low	398.7	30.2	259.4
	2.5	40	High	397.5	31.8	330.4
2-4	2.5	40	Low	398.9	25.8	34.5
	2.5	40	High	397.1	31.6	342.6
	2.5	40	Low	398.4	26.1	35.2
	2.5	40	High	397.5	31.4	338.7
2-4	2.5	40	Low	398.9	25.8	34.5
	2.5	40	High	397.1	31.6	342.6
	2.5	40	Low	398.4	26.1	35.2
	2.5	40	High	397.5	31.4	338.7
2-5	2.5	40	Low	398.2	29.7	125.4
	2.5	40	High	397.5	31.3	320.4
	2.5	40	Low	397.8	30.0	127.8
	2.5	40	High	397.6	31.0	321.7
2-6	2.5	40	Low	398.3	27.6	247.2
	2.5	40	High	397.8	30.4	318.5
	2.5	40	Low	397.8	30.5	264.8
	2.5	40	High	387.4	31.9	336.4

3.1. Interlayer Heterogeneity Experiments

The experimental results and the analysis of interlayer heterogeneity during waterflooding are presented. The study includes three core groups, each representing different permeability and contrast levels between the layers. These groups were designed to simulate various interlayer heterogeneity scenarios, allowing for a comprehensive assessment of how vertical permeability variations influence injected water distribution and sweep efficiency [8,42]. Table 2 presents the laboratory experimental results involving water injection modes for core groups with interlayer heterogeneities. The relationships between the injection water flow rate and water injection mode under different permeability ranges were plotted. Figure 5a–c show the relationship between the liquid volume produced in the layers versus injection time for the first 20 minutes for each core group. By analyzing the data obtained from the sand pack models configured with interlayer heterogeneities, we can understand how these variations influence the behaviour of the flooding process.

 doi:10.20944/preprints202412.0942.v1

Table 2. Experimental results injection modes in interlayer heterogeneous reservoirs.

Core	Injection mode	Permeability range x10^{-3} μm^2	Diameter cm	Length cm	Relative Permeability	Dry weight g	Porosity %	Permeability x10^{-3} μm^2	Original oil volume ml	Produced oil volume ml
2-1	Steady state	312.8	2.5	40	Low	398.8	26.0	35.7	51.1	14.6
			2.5	40	High	398	31.9	348.5	62.6	51.5
	Pulsating	303.0	2.5	40	Low	398.7	25.8	34.8	50.7	35.8
			2.5	40	High	398.1	31.5	337.8	61.9	55.7
2-2	Steady state	191.5	2.5	40	Low	398.4	30.3	127.4	59.5	37.5
			2.5	40	High	397.9	31.3	318.9	61.5	49.8
	Pulsating	196.3	2.5	40	Low	398.5	29.5	125.4	57.9	42.5
			2.5	40	High	398.3	31.0	321.7	60.9	53.8
2-3	Steady state	75.5	2.5	40	Low	398.9	29.4	251.8	57.7	44.5
			2.5	40	High	398.4	31.7	327.3	62.2	50.9
	Pulsating	71.0	2.5	40	Low	398.7	30.2	259.4	59.3	42.8
			2.5	40	High	397.5	31.8	330.4	62.4	52.0

The experimental results highlighted significant flow behaviour and sweep efficiency differences between steady-state and pulsating water injection modes, particularly in low-permeability cores. In steady-state flooding, high-permeability cores produced oil faster, while low-permeability cores exhibited delayed and lower output [41].

Figure 5a shows that in core group 2-1, with a 307.9 × 10^{-3} μm^2 permeability range, steady-state water flooding caused the high-permeability core to produce liquid immediately. In contrast, the low-permeability core only began producing liquid after 4 minutes. The high-permeability core showed a rapid rise in production, whereas the low-permeability core experienced a gradual increase over time. The high-permeability core contributed 89.7% of the total liquid production, whereas the low-permeability core accounted for only 10.3%.

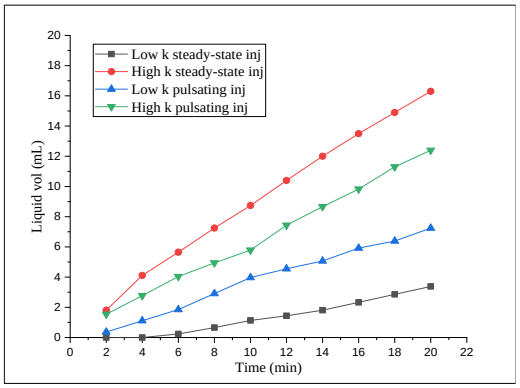

(**a**)

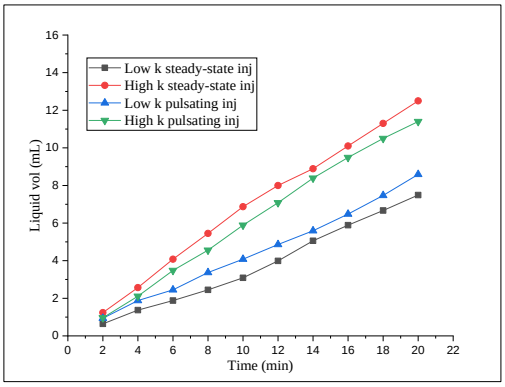

(**b**)

 doi:10.20944/preprints202412.0942.v1

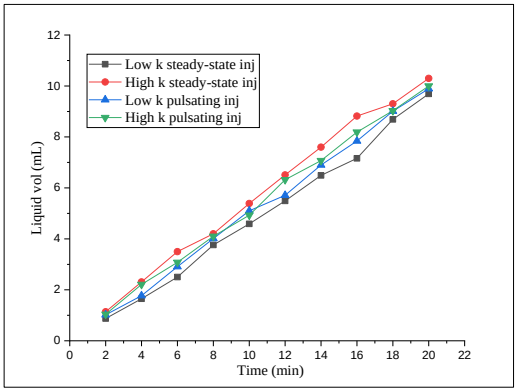

(c)

Figure 5. Interlayer heterogeneous core groups flow relationship (a) 2-1 core group flow relationship (b) 2-2 core group flow relationship (c) 2-3 core group flow relationship.

In pulsating water flooding, the high-permeability core started producing liquid immediately but at a slower rate than in steady-state flooding. The low-permeability core, however, began producing liquid earlier with pulsating injection and maintained a relatively steady production rate. As flooding continued, the liquid output from the low-permeability core increased substantially, producing a higher total volume than in steady-state conditions. The high-permeability core accounted for 65.5% of the total flow, while the low-permeability core contributed 34.5%. Compared to steady-state water flooding, the flow rate through the high-permeability core decreased by 24.2%, while the flow rate through the low-permeability core increased by 24.2%.

Figure 5b shows that in core group 2-2, with a permeability range of 193.9 × 10^{-3} μm² and steady-state flooding conditions, the high-permeability cores contributed 65.5% of the total flow, while the low-permeability cores accounted for the remaining 34.5%.

With pulsating flooding conditions, the flow distribution shifted, and both high- and low-permeability cores exhibited similar breakthrough times. However, the fluid production from the high-permeability core decreased to 57.1%, while the contribution from the low-permeability core increased to 42.9%, showing an 8.4% improvement compared to steady-state flooding. The shift demonstrates how pulsating injection improves flow balance by increasing the flow to low-permeability zones and reducing the dominance of high-permeability zones, thereby enhancing overall sweep efficiency.

Figure 5c shows that the flow distribution was more balanced in core group 2-3, with a permeability range of 73.25 × 10^{-3} μm². Under steady-state flooding, high-permeability cores contributed 54.4% of the total flow, while low-permeability cores contributed 45.6%. The liquid production curve for this core group was relatively compact, showing a narrow gap between high and low permeability curves. Fluid flow was observed in both high and low permeability cores from the beginning of displacement, with the flow rate remaining steady as displacement progressed. The fluid production from the high-permeability core was slightly higher than that from the low-permeability core, contributing a smaller portion of the total injection volume.

Under pulsating flooding conditions, the breakthrough times for high and low-permeability cores were similar to those observed during steady-state flooding. However, the distribution of liquid production shifted. The high-permeability core accounted for 51.0% of the total injected water, while the low-permeability core contributed 49.0%. This indicates that pulsating injection improved the flow balance, as the flow rate of the high-permeability core decreased by 3.4%, while the flow rate of the low-permeability core increased by 3.4%. This demonstrates how pulsating water injection can enhance flow in high and low permeability zones, leading to a more even distribution of the injected fluid.

Figure 6a shows the recovery relationship of interlayer heterogeneities core groups with the injection modes. The experimental results demonstrated that pulsating water flooding improved recovery rates for both high and low-permeability cores compared to steady-state water flooding

 doi:10.20944/preprints202412.0942.v1

[12,14,23,43]. In core group 2-1 under steady-state, the ultimate recovery rates were 82.2% for high-permeability cores and 28.6% for low-permeability cores. However, under pulsating water flooding, these rates increased to 90.1% for high-permeability cores and 70.7% for low-permeability cores, showing an improvement of 7.9% and 42.1%, respectively. In core group 2-2, the recovery rates under pulsating flooding were also higher than steady-state flooding. The recovery rate for high-permeability cores increased from 81.0% to 88.4%, and for low-permeability cores, rose from 63.0% to 73.4%. For core groups 2-3, pulsating water flooding also yielded higher recovery rates than steady-state flooding. High-permeability cores showed a recovery rate of 89.0%, while low-permeability cores showed 83.3% recovery under pulsating flooding. The recovery rates were 11.9% and 1.5% higher for high and low permeability cores under pulsating flooding than steady-state flooding.

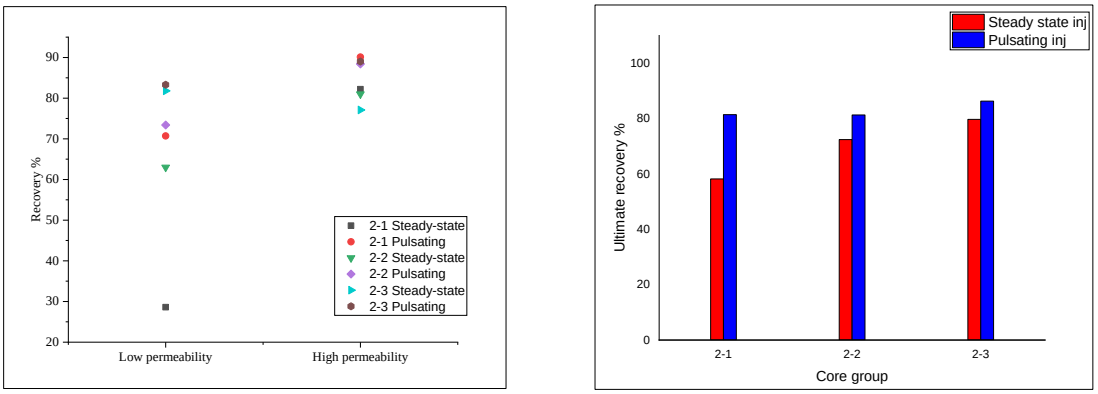

(**a**) (**b**)

Figure 6. Recovery relationships in interlayer heterogeneity (a) Core group relationship (b) Ultimate recovery of each group.

Figure 6b shows the ultimate recovery in each core group in interlayer heterogeneity experiments. It compares the total recovery across these groups with the injection modes. Pulsating water flooding enhanced the recovery factor in high- and low-permeability cores, with more significant improvements in low-permeability zones. For all groups of interlayer heterogeneous cores, the final recovery factors were higher for lower permeability layers under pulsating water flooding than steady-state flooding. This highlights the effectiveness of pulsating injection in improving sweep efficiency and boosting overall recovery. Pulsating water injection improved the ultimate recovery rate in interlayer heterogeneous simulation reservoirs, enhancing the overall effectiveness of water flooding. However, the degree of improvement varies depending on the permeability range of the core groups, emphasizing the critical role of permeability in the success of water flooding in interlayer heterogeneous reservoirs [18,42].

The permeability ranges for the three groups of interlayer heterogeneity simulation cores were 307.9×10^{-3} μm², 193.9×10^{-3} μm², and 73.25×10^{-3} μm², respectively. Under pulsating water flooding, the recovery efficiency increased by 23.2%, 8.9%, and 6.6%, respectively. These results highlight the greater effectiveness of pulsating water flooding in improving recovery, particularly for low-permeability cores, and demonstrate the variability in recovery rates across different core groups with varying permeability. The findings emphasize how pulsating injection can enhance oil recovery, especially in low permeability zones, while revealing different impacts across interlayer heterogeneous cores under different water injection modes.

3.2. Inlayer Heterogeneities Experiments

This section presents the experimental results and analysis of water flooding in intralayer heterogeneity reservoirs. The inlayer setup enables the investigation of fluid flow and oil displacement within a single layer with internal heterogeneity. It allows evaluation of how pulsating water injection affects displacement efficiency and flow behaviour across zones with varying

 doi:10.20944/preprints202412.0942.v1

permeability within the same stratigraphic layer. For the inlayer heterogeneity experiments, the outlets along the length of the sand packs models with high and low permeabilities were arranged in an inline configuration, as shown in Figure. 4. The laboratory experimental results involving injection modes for core groups with inlayer heterogeneities were organized and presented in Table 3.

Table 3. Experimental results for injection modes in intralayer heterogeneous reservoirs.

Core	Injection mode	Permeability range x10^{-3} μm^2	Diameter cm	Length cm	Relative Permeability	Dry weight g	Porosity %	Permeability x10^{-3} μm^2	Original oil volume ml	Produced oil volume ml
2-4	Steady state	308.1	2.5	40	Low	398.9	25.8	34.5	50.7	10.6
			2.5	40	High	397.1	31.6	342.6	62.0	53.7
	Pulsating	303.5	2.5	40	Low	398.4	26.1	35.2	51.2	24.5
			2.5	40	High	397.5	31.4	338.7	61.7	55.7
2-5	Steady state	195.0	2.5	40	Low	398.2	29.7	125.4	58.3	19.8
			2.5	40	High	397.5	31.3	320.4	61.5	51.4
	Pulsating	193.9	2.5	40	Low	397.8	30.0	127.8	58.9	28.7
			2.5	40	High	397.6	31.0	321.7	60.9	55.2
2-6	Steady state	71.3	2.5	40	Low	398.3	27.6	247.2	54.2	25.3
			2.5	40	High	397.8	30.4	318.5	59.7	49.8
	Pulsating	71.6	2.5	40	Low	397.8	30.5	264.8	59.7	30.7
			2.5	40	High	397.4	31.9	336.4	62.6	56.8

Figure 7a–c show the relationship between the liquid volume produced in the layers and injection time for each core group's first 20 minutes. By analyzing the data obtained from the sand pack models configured with intralayer heterogeneities, we can understand how these variations influence the behaviour of the flooding process.

Figure 7a shows the behaviour of the 2-4 core group with a 305.8 × 10^{-3} μm^2 permeability range under different injection modes. During steady-state flooding, the high permeability core exhibited immediate liquid production, with a significant increase in volume over time. Conversely, the low-permeability core began producing liquid only after 4 minutes, with a gradual rise in volume. The difference between the two curves indicates that the water inflow to the high-permeability core was much more significant, with the high-permeability core contributing 90.8% of the total inflow and the low-permeability core 9.2% during the first 20 minutes.

Both high and low-permeability cores showed liquid outflow during pulsating water drive conditions at the beginning of displacement. As water flooding continued, liquid production increased for both cores at different rates. The gap between the two curves indicates that, at any observed time, the injected water flow was higher for the high permeability core than the low permeability core. Over the first 20 minutes, the average partial flows were 67.2% for the high permeability core and 32.8% for the low permeability core.

 doi:10.20944/preprints202412.0942.v1

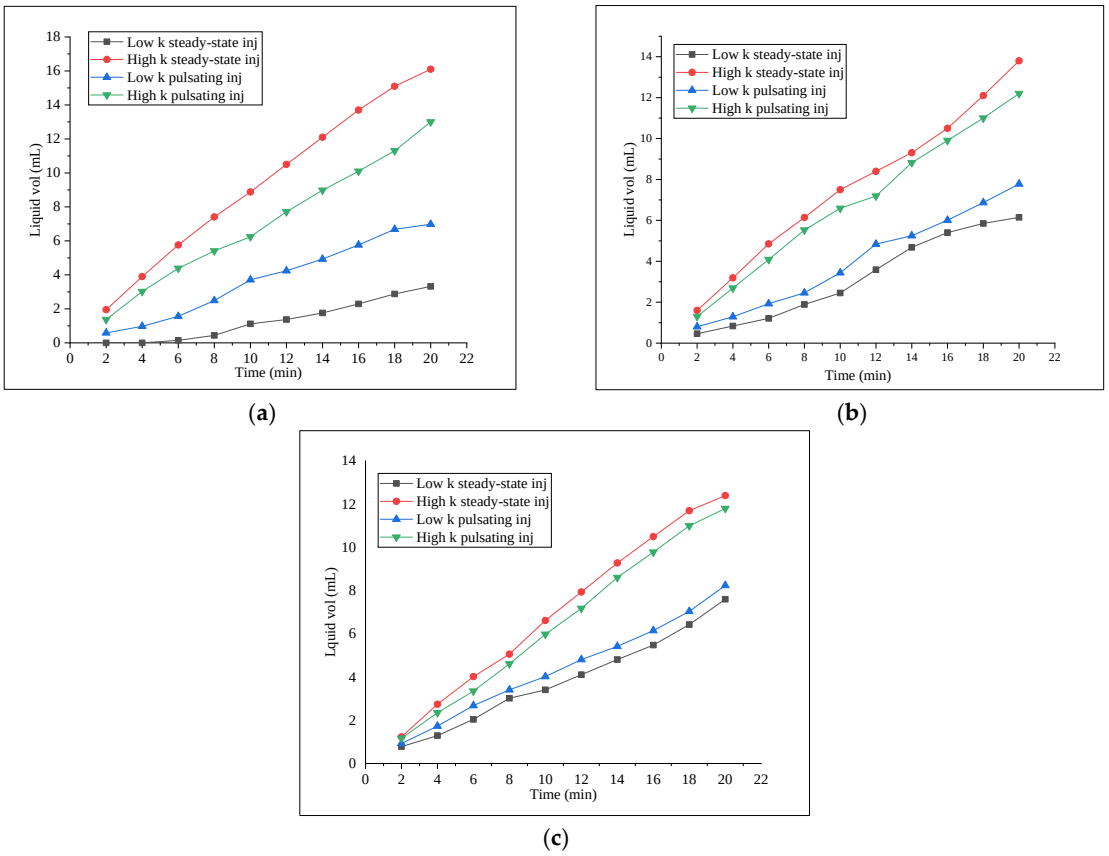

Figure 7. Inlayer heterogeneous core groups flow relationship (a) 2-4 core group flow relationship (b) 2-5 core group flow relationship (c) 2-6 core group flow relationship.

Figure 7b shows the behaviour of the 2-5 core group with the permeability range of 194.5 μm² under different injection modes. In the same water injection mode, liquid production in high and low-permeability cores differed at any observed time. Under steady-state water flooding, fluid flow was observed from high and low permeability cores at the beginning of water injection. Liquid production increased over time, with the high-permeability core showing a more significant increase than the low-permeability core. The difference between the two curves indicates that the water injection flow into the high permeability core was consistently higher than that into the low permeability core at any observed moment. In the first 20 minutes, the average partial flows were 72.2% for the high-permeability core and 27.8% for the low-permeability core.

Under pulsating water injection, the liquid was produced from both high and low-permeability cores from the beginning of water injection, with output showing a positive correlation with flooding time. The high-permeability core exhibited a faster rate of liquid production. Initially, the injected water flow was higher in the high-permeability core. Still, the gap between the two cores decreased over time, with average partial flow rates of 64.5% for the high permeability core and 35.5% for the low permeability core during the first 20 minutes. The pulsating water injection maintained relative stability, reducing the injected water flow in the high permeability core by 7.7% and increasing the injected water flow in the low permeability core by approximately 7.7%. Overall, the injected water flow for the high permeability core was lower under pulsating water drive than under steady-state conditions. In contrast, the opposite trend was observed for the low permeability core.

Figure 7c shows the behaviour of the 2-6 core group with a 71.5 × 10^{-3} μm² permeability range under different injection modes. During steady-state water flooding, liquid outflow was observed from the sand pack outlet for both high- and low-permeability cores, with initial production being similar for both. As water flooding continued, the gap between the two curves widened, indicating that water flow was higher for the high-permeability core than the low-permeability core.

This difference in flow rates suggests the formation of water channelling in the high-permeability core, where water preferentially flows through the path of least resistance, bypassing

 doi:10.20944/preprints202412.0942.v1

parts of the core and resulting in an uneven flow distribution. In contrast, the low-permeability core, with more uniform resistance, showed a slower, more consistent water distribution. In the first 20 minutes, the average partial flow rates for the high-permeability core were approximately 64.6% and 35.4%, respectively [20,44,45].

Under pulsating water injection, fluid production, output volume, and water injection time patterns were similar to those observed during steady-state water injection. However, compared to steady-state conditions, the liquid output was lower for the high-permeability core and higher for the low-permeability core under pulsating water injection at any observed time. The gap between the two curves indicated that while the injected water flow for the high-permeability core remained higher than for the low-permeability core, the difference was reduced under pulsating injection. During the first 20 minutes, the average partial flow rates were 58.8% for the high-permeability core and 41.2% for the low-permeability core.

Considering the entire experimental observation, the partial flow rate was uniform during the first 8 minutes due to the small permeability range and weak heterogeneity, resulting in a compact curve. However, after 8 minutes of water injection, the development of water channelling intensified the imbalance in partial flow, increasing the gap between the curves [20,38,44,45]. Within the experimental range, the injected water flow for the high-permeability core under pulsating water injection was lower than that under steady-state conditions. The injected water flow for the low-permeability core was higher under pulsating water drive than steady-state water injection. The pulsating water injection proved relatively stable, reducing the injected water flow for the high-permeability core by 5.8% and increasing the injected water flow for the low-permeability core by 5.8%.

Figure 8a shows the permeability and oil recovery relationship for the 2-4, 2-5, and 2-6 core groups under different water flooding modes. In the 2-4 core group, steady-state flooding resulted in recoveries of 20.9% for low permeability and 86.5% for high permeability. Pulsating flooding increased recoveries to 47.8% for low permeability and 90.3% for high permeability. The improvements were 26.9% for low permeability and 3.8% for high permeability at 306 × 10^{-3} μm² permeability.

In the 2-5 core group, steady-state recovery was 34.0% for low permeability and 83.6% for high permeability. Pulsating flooding increased recoveries to 48.7% for low permeability and 90.7% for high permeability. The improvement was greater in low permeability (14.7%) compared to high permeability (7.1%).

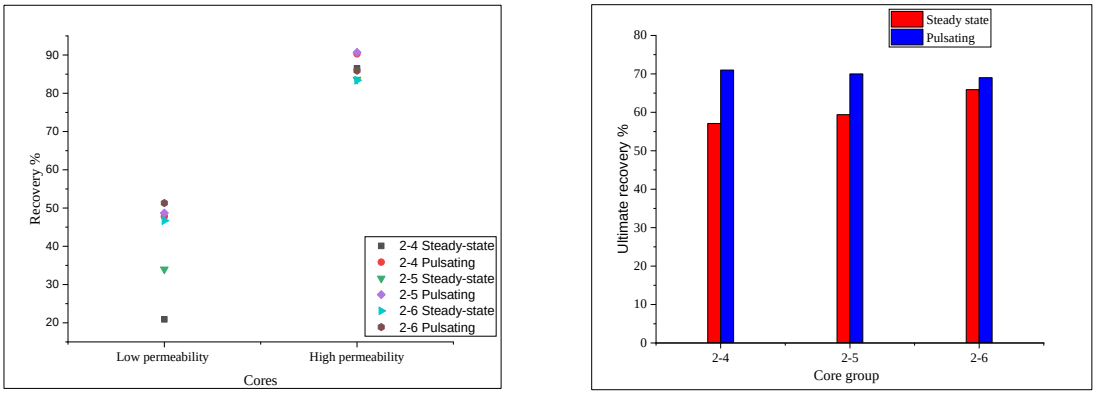

(**a**) (**b**)

Figure 8. Recovery relationships in inlayer heterogeneity (a) Core group relationship (b) Ultimate recovery of each group.

In the 2-6 core group, the steady-state recovery rate for the low-permeability core was 46.7% and 83.4% for the high-permeability core. Under pulsating flooding, these rates increased to 51.3% and 85.9%, showing improvements of 4.6% and 2.5%, respectively. Overall, pulsating water flooding

 doi:10.20944/preprints202412.0942.v1

enhanced recovery in high and low permeability cores, with more significant improvements in low permeability cores.

Figure 8b shows the final oil recovery for different water flooding modes based on experimental results for the 2-4, 2-5, and 2-6 core groups with intraformational heterogeneity. Under steady-state water flooding, the ultimate recovery factors were 57.1% for the 2-4 core group, 59.4% for the 2-5 core group, and 65.9% for the 2-6 core group. During pulsating water drive, recovery factors increased by 13.9%, 10.6%, and 3.1% for the 2-4, 2-5, and 2-6 core groups, respectively, indicating that pulsating water flooding enhanced recovery, especially in more heterogeneous reservoirs. These results demonstrate the significant influence of both water injection mode and reservoir heterogeneity on the comprehensive recovery efficiency, with pulsating water flooding leading to higher recovery in all core groups than steady-state flooding. The improvement in recovery was positively correlated with the reservoir's heterogeneity level, showing the benefits of pulsating water flooding for inlayer heterogeneous reservoirs.

3.3. Driving Mechanisms of Pulsating Water Flooding in Heterogeneous Reservoirs

In the initial phase of the experiment, pulsating flooding (represented by the green curve for high permeability and blue curve for low permeability) shows greater variability in total liquid production compared to steady-state flooding (black for low permeability and red for high permeability). This variability arises from the unique dynamics of pulsating flooding, where pulsations reduced water flow in high-permeability regions (green curve) and increased flow in low-permeability zones (blue curve). This led to a slowdown in liquid production in the high-permeability areas while enhancing fluid mobilization in low-permeability zones that would otherwise remain unswept under steady-state injection.

The initial fluctuations reflected a redistribution of flow, as the water was diverted from high-permeability areas (where it caused more water channelling and dominated the flow, as seen in the red curve) to improve recovery in lower-permeability regions (where pulsations led to higher oil recovery, as seen in the blue curve).

Over time, pulsating flooding becomes more effective. The long-term benefits are reflected in higher total oil recovery, as pulsating flooding improves displacement efficiency in low-permeability zones and reduces excessive water production in high-permeability areas. This results in more efficient oil recovery, as shown in Tables 2 and 3, where pulsating flooding (blue and green curves) outperforms steady-state flooding (black and red) in total oil recovery despite initial variability.

For steady-state water flooding, as the permeability ratio increases, the loss rate of sweep efficiency also increases, indicating that higher permeability heterogeneity leads to lower sweep efficiency. However, with pulsating water flooding, the trend reverses: while the loss rate increases with the permeability ratio in steady-state, it decreases under pulsating conditions, suggesting that pulsating injection mitigates the negative effects of permeability heterogeneity on sweep efficiency, as shown in Figure 9 [42].

Pulsating water flooding introduces vibrations that mobilize trapped non-wetting fluids in low-permeability regions. Once a critical acceleration threshold is reached, the fluid is displaced, restoring flow and enhancing permeability [46]. Studies of water flooding in reservoirs with interlayer and intraformational heterogeneity show that water injection mode and reservoir heterogeneity influence the effectiveness of water drive. High permeability cores exhibited higher flow rates and recovery efficiencies than low permeability cores, but this difference narrowed as the permeability range decreased. Pulsating injection generates pressure oscillations that induce cross-flow between layers with different permeabilities, facilitating fluid movement from low-permeability to higher-permeability areas and mobilizing trapped oil. Though the pressure effects of pulsations are small, the induced rock stress significantly improves oil recovery, especially in heterogeneous reservoirs [23].

Even small transient stresses can play a role in fluid mobilization during pulsating water flooding. Laboratory and field studies have demonstrated that stresses as low as 1 MPa, which are too small to cause shear failure or create new fractures, can significantly alter permeability and fluid

 doi:10.20944/preprints202412.0942.v1

flow. These minor transient stresses, generated by pressure oscillations from pulsating flooding, improve fluid displacement by altering pore pressure and flow dynamics. Such transient stresses increase vertical sweep efficiency, especially in heterogeneous reservoirs where conventional flooding methods fail to reach low-permeability zones. This further supports the observed improvements in recovery, as pulsating water flooding redistributes oil from areas that would otherwise remain bypassed due to permeability differences [24].

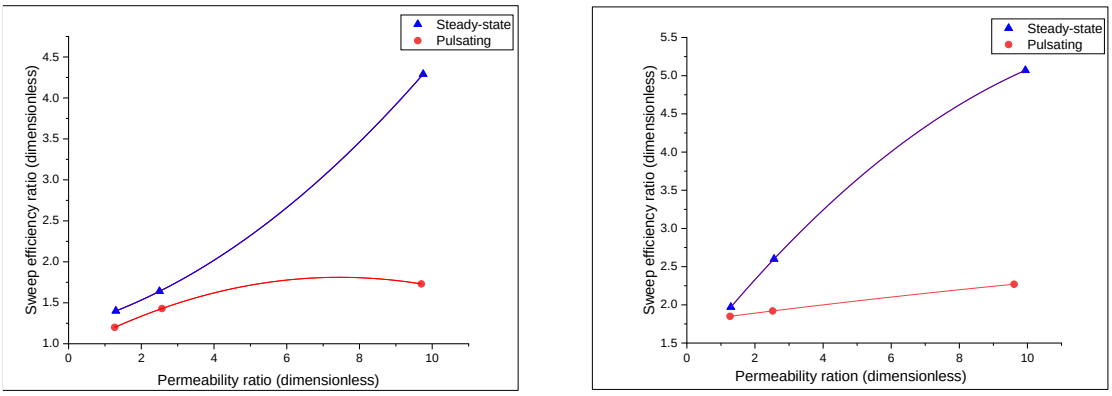

(**a**) (**b**)

Figure 9. The curve between sweep efficiency recovery ratio and permeability ratio (a) interlayer heterogeneity (b) Inlayer heterogeneity.

Figure 10 shows cross-flow between high and low permeability layers, where fluid moves across layers with differing permeabilities. As water flows through more porous layers, it displaces fluids in adjacent, less permeable layers, driven by interface pressure differences [47]. Under pulsating water flooding, the injected water flow rate in high-permeability cores was lower compared to steady-state conditions, with this reduction becoming more pronounced as permeability increased. Conversely, the injected water flow rate in low-permeability cores was higher under pulsating conditions than under steady-state, with the increase becoming more significant as the permeability range widened. Despite the higher flow rates in low-permeability cores, recovery efficiency in high-permeability cores remained superior.

However, the overall recovery rate for all core groups under pulsating water flooding was higher than under steady-state flooding, with improvements positively correlated with the permeability range. Pulsating water injection led to more uniform water distribution, enhancing recovery in vertically heterogeneous reservoirs. Overall, pulsating water drive proved more effective than steady-state, particularly in reservoirs with significant permeability variation.

Pulsating water flooding, influenced by external mechanical waves, introduces instabilities in the velocity field across the system. Unlike conventional water flooding, where flow is more stable, pulsations enhance these instabilities, particularly in the longitudinal and transverse directions. While pulsating waterflooding does not reduce the fingering caused by viscosity contrasts, it amplifies it, extending the fingers of the displacing fluid into previously bypassed regions, including low-permeability or high-viscosity zones. This behaviour enhances ultimate recovery by enabling the fluid to reach areas that remain untapped in conventional flooding. Vibration stimulation is especially useful in depleted reservoirs, where it helps mobilize fluids from hard-to-reach zones, improving overall sweep efficiency [48].

Pulsating waterflooding, driven by pressure fluctuations, enhances oil recovery in reservoirs with low- and high-permeability zones. These pressure variations help redistribute oil and reduce residual oil saturation by mobilizing trapped oil in low-permeability areas. The periodic pressure pulses deform pore walls, altering the pore structure and improving fluid flow, thus increasing sweep efficiency and recovery rates [49]. Additionally, pulsating waterflooding encourages oil ganglia coalescence, forming larger, more mobile oil clusters that flow more easily through the reservoir. The pressure pulses also alter rock wettability, facilitating better oil migration [49].

 doi:10.20944/preprints202412.0942.v1

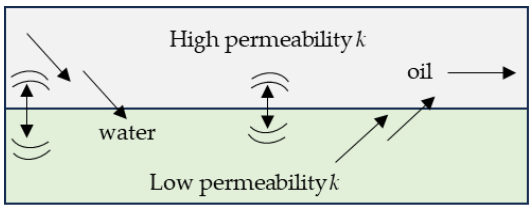

Figure 10. Crossflow between high and low permeability layers.

In this study, we observe that the increased oil production from pulsating waterflooding is likely due to an improvement in Vertical Sweep Efficiency (VSE) rather than the direct mobilization of waterflood residual oil. VSE, which measures how effectively injected water displaces oil, is influenced by mobility ratio, water-oil ratio, and permeability variations. A high mobility ratio and significant permeability contrasts are known to reduce VSE, as water can bypass oil in less permeable layers, leading to poor sweep efficiency. Pulsating waterflooding appears to address this challenge by introducing pressure fluctuations that disrupt the flow patterns within the reservoir, promoting more uniform oil displacement. This method is particularly effective in reservoirs with high permeability heterogeneity, where steady-state flooding tends to be less effective.

The first observation suggests that the improvement in oil production is not simply due to the mobilization of residual oil but rather to a more effective sweep of oil that had been bypassed due to reservoir heterogeneity. By enhancing the vertical sweep, pulsating waterflooding ensures that water reaches previously inaccessible or poorly swept zones, thereby increasing the overall recovery. This is consistent with the understanding that the primary benefit of pulsating waterflooding lies in optimizing the distribution of injected water throughout the reservoir, leading to more effective oil displacement.

We find that pore pressure oscillations produced by pulsating waterflooding lead to transient increases in the flow rate [50]. This further supports the idea that the pressure fluctuations improve the sweep efficiency. A possible explanation for this improvement is the hypothesis that low-frequency vibrations generated during pulsating waterflooding could mobilize oil ganglia trapped in rock pores. These vibrations might create local pressure gradients or fluctuate oil-water interfaces, dislodging trapped oil and improving flow dynamics. While high-frequency vibrations have limited penetration depth and may not significantly affect the reservoir, researchers such as Nikolaevskiy and colleagues propose that low-frequency vibrations could induce high-frequency waves through rock grain movements. This, in turn, could alter oil-water relative permeabilities, allowing injected water to more effectively displace trapped oil and ultimately improve recovery.

4. Conclusions

This study evaluated the impact of pulsating water injection on reservoirs with interlayer and inlayer heterogeneity, demonstrating that the effectiveness of water flooding depends on both the injection method and the degree of reservoir permeability variation. Many reservoirs, especially in China, have irregular permeability profiles that cause uneven water distribution, early water breakthroughs, and low oil recovery with conventional methods. Pulsating water injection addresses these issues by redistributing injected water more evenly, reducing flow in high-permeability zones, and improving sweep efficiency and oil displacement in low-permeability areas. In reservoirs where early water breakthroughs have already occurred, pulsating water injection proves particularly effective. The periodic pressure variations introduced by pulsating injection disrupt established preferential flow paths, mitigating further water breakthroughs and preventing additional oil bypassing. This method redistributes water more evenly across the reservoir, enabling it to reach unswept low-permeability zones and recover oil that would otherwise remain trapped.

Pulsating water injection significantly enhances recovery during the initial flooding phase by improving sweep efficiency under challenging conditions. In interlayer heterogeneity, pulsating water injection improved total recovery by 23.2%, 8.9%, and 6.6% for core groups with permeability ranges of 307.9×10^{-3} μm², 193.9×10^{-3} μm², and 73.25×10^{-3} μm², respectively. Similarly, in inlayer

 doi:10.20944/preprints202412.0942.v1

heterogeneity, the recovery increased by 13.9%, 10.6%, and 3.1% for core groups 2-4, 2-5, and 2-6, respectively. Pulsating water injection increases overall recovery and enables operators to optimize flooding parameters, extending reservoir productivity. By improving water distribution and oil recovery, pulsating injection offers a cost-effective and scalable solution for managing heterogeneous sandstone reservoirs and achieving enhanced long-term recovery efficiency. This approach proves particularly beneficial in reservoirs with significant permeability contrasts, providing a robust strategy for improving oil recovery and optimizing waterflooding performance.

Author Contributions: Conceptualization, O.M. and P.C.; methodology, O.M. and P.C.; investigation, O.M.; writing—original draft preparation, O.M.; writing—review and editing, P.C. All authors have read and agreed to the published version of the manuscript.

Funding: The Natural Science Foundation of China sponsored this research," grant number 51874339 and 51904320

Data Availability Statement: The datasets used and/or analyzed during the current study are available from the corresponding author upon reasonable request.

Conflicts of Interest: The authors declare no conflicts of interest.

References

1. Ibrahim, A. S. Investigation of the mobilization of residual oil using micromodels. In Proceedings of SPE Annual Technical Conference and Exhibition, OnePetro, New Orleans, Louisiana, October 2009. [CrossRef]
2. Xu, Z. X.; Li, S. Y.; Li, B. F.; Chen, D. Q.; Liu, Z. Y.; Li, Z. M. A review of development methods and EOR technologies for carbonate reservoirs. *Pet. Sci*. **2020,** 17, 990–1013. [CrossRef]
3. Manrique, E.; Thomas, C.; Ravikiran, R.; Izadi, M.; Lantz, M.; Romero, J.; Alvarado, V. Current status and opportunities. In Proceedings of SPE Improved Oil Recovery Symposium, OnePetro, Tulsa, Oklahoma, USA, April 2010. [CrossRef]
4. Kazemzadeh, Y.; Shojaei, S.; Riazi, M.; Sharifi, M. Review on application of nanoparticles for EOR purposes: A critical review of the opportunities and challenges. *Chinese J. Chem. Eng*. **2019**, 27, 237–246. [CrossRef]
5. Tan, Y.; Zhang, Y.; Hui, C.; Yu, C.; Tian, S.; Wang, T.; Wang, F. Resonance-Enhanced Pulsing Water Injection for Improved Oil Recovery: Micromodel Experiments and Analysis. *Processes*. **2023**, 11, 957. [CrossRef]
6. Wang, K.; Zheng, W.; He, Y.; Tang, C.; Pan, Y.; Li, J.; Jiang, J.; Cai, S.; Li, J. Analysis of Inter-Layer Interference in Multi-Layer Reservoir Commingled Production Wells. *Processes.* **2024**, 12, 1–14. [CrossRef]
7. Zhang, Z.; Gan, H.; Zhang, C.; Jia, S.; Yu, X.; Zhang, K.; Zhong, X.; Zheng, X.; Shen, T.; Qu, L.; Zhang, R. Experimental Study on Improving Oil Recovery Mechanism of Injection–Production Coupling in Complex Fault-Block Reservoirs. *Energies*. **2024**, 17, 1505. [CrossRef]
8. Zhao, L.; Li, L.; Wu, Z.; Zhang, C. Analytical model of waterflood sweep efficiency in vertical heterogeneous reservoirs under constant pressure. *Math. Probl. Eng*. **2016**, 10, 1–9. [CrossRef]
9. Li, M.; Qu, Z.; Wang, M.; Ran, W. The Influence of Micro-Heterogeneity on Water Injection Development in Low-Permeability Sandstone Oil Reservoirs. *Minerals*. **2023**, 13, 1533. [CrossRef]
10. Liu, Y.; Luo, X.; Kang, K.; Li, T.; Jiang, S.; Zhang, J.; Zhang, Z.; Li, Y. Permeability characterization and directional wells initial productivity prediction in the continental multilayer sandstone reservoirs: A case from Penglai 19-3 oil field, Bohai Bay Basin. *Pet. Explor. Dev*. **2017**, 44, 97–104. [CrossRef]
11. Weimann, P. A.; Sanchez, A.; Espinosa-Vázquez, L. A.; Davidson, B.; Martinez, R. G. Effective Well Stimulation Using Fluid Pulsing to Inject Surfactant Solutions. In Proceedings of Heavy Oil Latin America Conference & Exhibition, Puerto Vallarta, Mexico, 2013
12. Al-Shalabi, E. W.; Ghosh, B. Effect of Pore-Scale Heterogeneity and Capillary-Viscous Fingering on Commingled Waterflood Oil Recovery in Stratified Porous Media. *J. Pet. Eng*. **2016**, 1–14. [CrossRef]
13. Xue, L.; Liu, P.; Zhang, Y. Status and Prospect of Improved Oil Recovery Technology of High Water Cut Reservoirs. *Water*. **2023**, 15, 1342. [CrossRef]
14. Yang, H.; Lao, J.; Tong, D.; Song, H. Numerical Investigation on EOR in Porous Media by Cyclic Water Injection with Vibration Frequency. *Water*. **2022**, 14, 3961 [CrossRef]
15. Mai, A.; Kantzas, A. Heavy oil waterflooding: Effects of flow rate and oil viscosity. *J. Can. Pet. Technol*. **2009,** 48, 42–51. [CrossRef]
16. Rostami, P.; Sharifi, M.; Aminshahidy, B.; Fahimpour, J. The effect of nanoparticles on wettability alteration for enhanced oil recovery: micromodel experimental studies and CFD simulation. *Pet. Sci.* **2019**, 16, 859–873. [CrossRef]

17. Groenenboom, J.; Wong, S.-W.; Meling, T.; Zschuppe, R.; Davidson. B. Pulsed Water Injection during water flooding. In Proceedings of SPE International Improved Oil Recovery Conference in Asia Pacific, OnePetro, Kuala Lumpur, Malaysia, October 2003. [CrossRef]
18. Hu, L. Z.; Sun, L.; Zhao, J. Z.; Wei, P.; Pu, W. F. Influence of formation heterogeneity on foam flooding performance using 2D and 3D models: an experimental study. *Pet. Sci*. **2020**, 17, 734–748. [CrossRef]
19. Spanos, T.; Davidson, B.; Dusseault, M.; Shand, D.; Samaroo, M. Pressure pulsing at the reservoir scale: A new IOR approach. *J. Can. Pet. Technol*. **2003**, 42, 16–27. [CrossRef]
20. A. Sivrikoz. Enhance Oil Recovery Modelling Using a Pressure Pulse-Geomechanical Black Oil Simulator. PhD, University of Alberta, Canada, 2009.
21. Zhu, T.; Xutao, H.; Vajjha, P. Downhole Harmonic Vibration Oil-Displacement System: A New IOR Tool. In Proceedings of SPE Western Regional Meeting, OnePetro, Irvine, California, March 2005. [CrossRef]
22. Gale, T. A Field and Numerical Investigation of the Pressure Pulsing Reagent Delivery Approach. Masters, University of Waterloo, Canada, 2011
23. C. Huh. Improved oil recovery by seismic vibration: A preliminary assessment of possible mechanisms. In Proceedings of SPE International Oil Conference and Exhibition in Mexico, OnePetro, Cancun, Mexico, August 2006. [CrossRef]
24. Elkhoury, J. E.; Brodsky, E. E.; Agnew, D. C. Seismic waves increase permeability. *Nature*, **2006**, 441, 1135–1138. [CrossRef]
25. Kalinski, M. E. Effect of Vibroseis Arrays on Ground Vibrations: A Numerical Study Effect of Vibroseis Arrays on Ground Vibrations: A Numerical Study. *J. Environ. Eng. Geophys*. **2007**, 12, 281–87. [CrossRef]
26. Guo, X.; Du, Z.; Li, G.; Shu, Z. Oilfield. High-Frequency Vibration Recovery Enhancement Technology in the Heavy Oil Fields of China. In Proceedings of SPE International Thermal Operations and Heavy Oil Symposium and Western Regional Meeting, OnePetro, Bakersfield, California, March 2004. [CrossRef]
27. Davidson, B. Fluid-Pulse Technology Boosts Oil Recovery. *J. Pet. Technol*. **2013**, 65, 34–35. [CrossRef]
28. Kostrov, S.; Wooden, W. Possible Mechanisms and Case Studies for Enhancement of Oil Recovery and Production Using In-Situ Seismic Stimulation. In Proceedings of SPE Symposium on Improved Oil Recovery, OnePetro, Tulsa, Oklahoma, USA, April 2008. [CrossRef]
29. Atamanchuk, I. Pressure Pulsing Potential During Waterflooding and CO2 Flooding of Heavy Oil Reservoirs. Masters, University of Regina, Canada, 2014.
30. Wang, J.; Dusseault, M. B. Fluid enhancement under liquid pressure pulsing at low frequency. In Proceedings of 7th Unitar International Conference on Heavy Crude and Tar Sands, Beijing, 1998.
31. Yan, W.; Sun, J.; Zhang, J.; Golsanami, N.; Hao, S. A novel method for estimation of remaining oil saturations in water-flooded layers. *Interpretation*. **2017,** 5, SB9-23. [CrossRef]
32. Amro, M.; Al-Mobarky, M.; Al-Homadhi, E. Improved Oil Recovery by Application of Ultrasound Waves to Waterflooding. In Proceedings of SPE Middle East Oil and Gas Show and Conference, OnePetro Manama, Bahrain, March 2007. [CrossRef]
33. Hamida, T.; Babadagli, T. Capillary Interaction of Different Oleic and Aqueous Phases Between Matrix and Fracture Under Ultrasonic Waves. In Proceedings of the SPE Europec/EAGE Annual Conference, OnePetro: Madrid, Spain, 13th June 2005. [CrossRef]
34. Hamida, T.; Babadagli, T. Effect of ultrasonic waves on the capillary-imbibition recovery of oil. In Proceedings of SPE Asia Pacific Oil and Gas Conference and Exhibition, OnePetro: Jakarta, Indonesia, April, 2005. [CrossRef]
35. Iassonov, P. P.; Beresnev, I. A. Mobilization of entrapped organic fluids by elastic waves and vibrations. *SPE J*. **2008**, 13, pp. 465–473. [CrossRef]
36. Yeganeh, M.; Hegner, J.; Lewandowski, E.; Mohan, A.; Lake, L.W.; Cherney, D.; Jusufi, A.; Jaishankar, A. Capillary Desaturation Curve Fundamentals. In Proceedings of SPE Improved Oil Recovery Conference, OnePetro: Tulsa, Oklahoma, USA, April 2016. [CrossRef]
37. Zheng, W.; Wang, K.; Li, J.; Jiang, J.; Tang, C.; He, Y.; Guan, Y.; Li, J. A Study on the Mechanism and Influencing Factors of Interlayer Injection–Production Coupling in a Heterogeneous Sandstone Reservoir. *Processes*. **2024**, 12. [CrossRef]
38. Gong, Q.; Liu, Z.; Zhu, C.; Wang, B.; Jin, Y.; Shi, Z.; Xie, L.; Wu, J. Heterogeneity of a Sandy Conglomerate Reservoir in Qie12 Block, Qaidam Basin, Northwest China and Its Influence on Remaining Oil Distribution. *Energies*. **2023**, 16, 2972. [CrossRef]
39. Rashid, B.; Muggeridge, A. H.; Bal, A.; Williams, G. Quantifying the impact of permeability heterogeneity on secondary-recovery performance. *SPE J*. **2012**, 17, pp. 455–468. [CrossRef].
40. Salimi, H.; Bruining, J. The influence of heterogeneity, wetting, and viscosity ratio on oil recovery from vertically fractured reservoirs. *SPE J*. **2011**, 16, pp. 411–428. [CrossRef]
41. Zhan, L.; Kuchuk, F.; Ma, S. M.; Al-Shahri, A. M.; Ramakrishnan, T. S.; Altundas, Y. B.; Zeybek, M.; Manin, Y.; Tartaras, E.; de Loubens, R.; Chugunov, N. Characterization of reservoir heterogeneity through fluid movement monitoring with deep electromagnetic and pressure measurements. *SPE J*. **2010,** 6, pp. 509–522. [CrossRef]

42. an, G.; Rui, S.; Fang, Z.; Baojiang, D.; Jingnan, Z. Research on Waterflood Sweep Law in Low Permeability Vertical Heterogeneous Reservoir. *Int. J. Digit. Content Technol. its Appl*. **2013,** 7, pp. 698–705. [CrossRef]
43. Meng, X.; Zhang, Q.; Dai, X.; Xue, S.; Feng, X.; Zhang, Y.; Tu, B.; Li, X. Experimental and simulation investigations of cyclic water injection in low-permeability reservoir. *Arab. J. Geosci*. **2021**, 14. [CrossRef]
44. Liu, Y.; Nie, F.; Zhang, B.; Liu, T.; Hong, Y. The Three-Dimensional Heterogeneous Simulation Study of CO2 Flooding in Low-Permeability Reservoirs. *Processes*. **2024,**12, p. 1843. [CrossRef]
45. Avagnina, N.; Segura, R. J.; Muniategui, M. E.; Sanchez Lona, A.; Keshka, A.; Kolli, K. R.; Wegmann-Sanchez, J. An Innovative Waterflood Optimization Method for Unconsolidated Sandstone Reservoirs to Increase Oil Production, Lower Water-Cut, and Improve or Stabilize Base Oil Decline Rate. In Proceedings of Pan American Mature Fields Congress, Veracruz, Mexico, 2015.
46. Beresnev, I.; Gaul, W.; Vigil, R. D. Direct pore-level observation of permeability increase in two-phase flow by shaking. *Geophys. Res. Lett*. **2011**, 38, pp. 2–6. [CrossRef]
47. Jeong, C.; Kallivokas, L. F.; Huh, C.; Lake, L. W. Estimation of oil production rates in reservoirs exposed to focused vibrational energy. In Proceedings of SPE Improved Oil Recovery Symposium, OnePetro, Tulsa, Oklahoma, USA, April 2014. [CrossRef]
48. Vogler, E. T.; Chrysikopoulos, C. V. Experimental investigation of acoustically enhanced solute transport in porous media. *Geophys. Res. Lett.* **2002**, 29, pp. 2–5. [CrossRef]
49. Sun, Q.; Retnanto, A.; Amani, M. Seismic vibration for improved oil recovery: A comprehensive review of literature. *Int. J. Hydrogen Energy*. **2020**, 45, pp. 14756–14778. [CrossRef]
50. Elkhoury, J. E.; Niemeijer, A.; Brodsky, E. E.; Marone, C. Laboratory observations of permeability enhancement by fluid pressure oscillation of in situ fractured rock. *J. Geophys. Res*. **2011,** 116, pp. 1–15. [CrossRef]